4

Thermal Contact and Thermal Isolation

In any low-temperature apparatus it is necessary to couple some parts thermally very well, whereas other parts have to be well isolated from each other and, in particular, from ambient temperature. The transfer of "heat" (or better "cold") and the thermal isolation are essential considerations when designing a low-temperature apparatus. These problems become progressively more acute at lower temperatures, and they will be discussed in this chapter. A general treatment of the thermal conductivity of materials is given in Sect. 3.3. Besides learning how to take advantage of the very different thermal conductivities of various materials, we have to discuss how to design an apparatus to achieve the desired goals. For example, there are situations, as in low-temperature calorimetry, where two substances have to be in good thermal contact and then have to be very well thermally isolated from each other for the remainder of the experiment. For this purpose we need a thermal switch and I shall place special emphasis on the discussion of superconducting heat switches which dominate the temperature range below 1 K. One of the severest problems in low-temperature technology is the thermal boundary resistance between different materials. This is a particularly severe problem if good thermal contact between liquid helium and a solid is required, as it will be discussed in the final sections of the present chapter.

The nuisance heat transfer by conduction and radiation will be considered at the beginning of Chap. 5. The various heat sources will be treated in Sects. 5.1.2 and 10.5, in connection with refrigeration to extremely low temperatures, where they can be particularly detrimental.

4.1 Selection of the Material with the Appropriate Cryogenic Thermal Conductivity

The low-temperature thermal conductivity of different materials can differ by many orders of magnitude and, fortunately, the thermal conductivity of the same material can even be varied by a great amount just by changing

the number of defects or impurities in it (Fig. 3.19). Hence, one has to be careful in selecting the right material for a low-temperature apparatus. The low-temperature thermal conductivities of various materials commonly in use in low-temperature equipment are exhibited in Figs. 3.19–3.24 and are listed in Table 3.2.

For *good thermal conductivity* the right choices are Cu (but: soft; nuclear specific heat at $T < 0.1$ K (Sect. 3.1.6 and Fig. 3.11), Ag (but: soft; expensive) or Al (but: soft, superconducting below 1 K; soldering only possible in an elaborate process, see Sect. 4.2.2). The highest practical conductivities of these metals are $\kappa \approx 10\,T$ [W K^{-1} cm^{-1}] if they are very pure; more typical is $\kappa \approx T$ [W K^{-1} cm^{-1}].

For *thermal isolation* the right choices are either plastics (Teflon, Nylon, Vespel, PMMA, etc.), graphite (careful, there exists a wide variety), Al$_2$O$_3$, or thin-walled tubing from stainless steel (but: soldering or silver brazing only with aggressive flux, which should be washed off very thoroughly; better is welding) or from Cu$_{0.7}$Ni$_{0.3}$ (easy to solder). However, the last two can be slightly magnetic at low temperatures (see Sect. 3.4.1) and can interfere with sensitive magnetic experiments. In general, glasses or materials composed of small crystallites (for phonon scattering) and containing a lot of defects and impurities (for electron scattering) are good thermal insulators. For example, the thermal conductivity of quartz glass at 1 K is only about 1% of that of crystalline quartz at the same temperature. The lowest thermal conductivity, $\kappa \cong 5 \times 10^{-6} T^{1.8}$ [W K^{-1} cm^{-1}] has been observed for AGOT nuclear graphite (Figs. 3.21 and 3.23).

If other properties do not matter too much, aluminium alloys or brass should be used because of their relatively low prices and, above all, because they can be easily machined. If tubes are employed which are filled with liquid ^{3}He, ^{4}He or an isotopic helium mixture, then the conductivity of the helium – which may be rather large (Sects. 2.3.4 and 2.3.6 and Figs. 2.12, 2.17, and 2.18) – usually dominates. The effect can be reduced by using capillaries with a small diameter to reduce the mean free path of the liquid's atoms.

In each low-temperature apparatus one needs *wires* to carry signals from room temperature to the low-temperature part, and back. For low-current leads thin Constantan ($\rho_{300\,\mathrm{K}} = 52.5\,\mu\Omega$ cm, $\rho_{4\,\mathrm{K}} = 44\,\mu\Omega$ cm) or Manganin ($\rho_{300\,\mathrm{K}} = 48\,\mu\Omega$ cm, $\rho_{4\,\mathrm{K}} = 43\,\mu\Omega$ cm) wires should be used because of their low thermal conductivity and the small temperature dependence of their electrical resistivity. However, one has to take into account the increase of their electrical resistance and of their specific heat due to magnetic contributions at $T < 1$ K (Fig. 3.9). This effect is smaller for PtW which has become a favorite heater wire for very-low-temperature applications; here the increase in specific heat due to a minute amount of magnetic impurities starts only below 0.1 K (Fig. 3.9). If large electrical currents – for example, for superconducting magnets – have to be carried to the low-temperature part, the advantage gained by using a good conductor and a large wire diameter to reduce Joule heating, and the disadvantage of the then increased thermal conductivity have to be

carefully considered. Often one may end up using Cu wires. Of course, then a proper heat sinking of the wires at various places on their way to low temperatures is of even greater importance. The optimum dimensions of leads carrying large currents into a cryostat were discussed in [4.1–4.6] (see also Sect. 13.4). At $T < 1\,\mathrm{K}$ the use of superconducting wires with their vanishing thermal conductivity for $T \to 0$ (Sects. 3.3.4, 4.2.2) is the right choice. Often it is adequate just to cover a Manganin or Constantan wire with a thin layer of superconducting solder ($T_\mathrm{c} \simeq 7\,\mathrm{K}$, see later) to have a lead with low thermal conductivity but zero electrical resistance. At $T < 0.1\,\mathrm{K}$ one can use monofilamentary NbTi without Cu or even without a CuNi matrix if the lowest possible thermal conductivity is required. In extreme cases the fine filaments of multifilament superconducting wires can be used, but soft soldering to these wires is not possible, so spot-welding or squeeze contacts are necessary [4.6, 4.7]; these techniques require some practice before they can be applied reliably. If the joint does not have to be superconducting then one can remove the Cu coating with concentrated HNO_3 except at the ends of the wire where the solder joints have to be made. An even better method is to coat the superconducting wire electrolytically with a layer of Cu (use $1\,l$ H_2O with at least $200\,\mathrm{g}$ $CuSO_4$, $27\,\mathrm{cm^3}$ H_2SO_4, and a current density of about $40\,\mathrm{mA\,mm^{-2}}$ between NbTi cathode and Cu anode). The same electrolytic process can be applied to cover stainless-steel tubing with a Cu layer to make the subsequent soldering easier. Phillip et al. [4.8] have described two techniques for joining multifilamentary superconducting NbTi wires. These joints have achieved critical currents in vacuum at $4.2\,\mathrm{K}$ comparable to the short segment ratio given by the manufacturer for the wires.

Wires for mesurements of small signals have to be twisted pairwise on their way in the cryostat, rigidly fixed and well shielded to keep pick-up signals low (Sect. 12.5). The design of coaxial cryogenic cables and the proper heat-sinking of leads will be discussed in Sect. 13.3.

4.2 Heat Switches

4.2.1 Gaseous and Mechanical Heat Switches

The simplest way to thermally connect and disconnect various parts of a low-temperature apparatus is to use a gas (at such a pressure that it does not condense at the temperatures involved) for thermal coupling and then remove it by pumping. This method is often employed in precooling the inner parts of a cryostat to LN_2 or LHe temperatures (Chap. 5). A gas pressure of 10^{-4} bar is sufficient for an adequate heat transfer. But usually many hours of pumping are then required to reduce the gas pressure for sufficient thermal isolation. The temperature at every place in the cryostat has to be above the condensation temperature of the gas so that efficient pumping is possible. If the exchange gas has not been pumped to a low enough pressure, time-dependent

heat leaks due to a continuing desorption and condensation of the remaining gas at the coldest surfaces may result (Sects. 5.1.2 and 10.5.3).

For ^{4}He, the superfluid film contributes to the heat transfer, too. For thermal isolation, ^{4}He has to be pumped very well to make sure that there is not enough of it left to form an unsaturated superfluid film if $T < 2.2$ K (Sect. 2.3.5). The advantage of H_2 as an exchange gas is the fact that it can be totally condensed out ("cryo-pumping") when liquid helium is transferred into the cryostat, so that time-consuming pumping can be avoided. However, one has to remember that the remaining H_2 molecules may undergo ortho–para conversion, giving rise to substantial heating (Sect. 2.2). As a conclusion, ^{3}He with its high vapour pressure, absence of exothermic reaction, and absence of superfluidity in the Kelvin temperature range, is the safest exchange gas for thermal contact.

Heat switches using liquid ^{4}He or ^{3}He have been described in [4.9–4.11]. The sealed ^{3}He gas heat switch of [4.11] uses a small charcoal pump to adsorb or desorb ^{3}He to create the gas pressure for switching between the "on" and "off" states. The thermal conductivity then changes by more than two orders of magnitude (from below 0.1 mW/K to several 10 mW/K) in the temperature range 0.5–3 K for the chosen design.

For many purposes, for example for calorimetry at $T > 1$ K, a mechanical heat switch is adequate. Thermal contact is made by metallic, usually gold-plated contacts pressed together mechanically (see below). Here the "open" state really is open, with no residual heat flow. Conductances of 1 mW K^{-1} in the low Kelvin range are typical for the closed state (Sect. 4.3.1) [4.1, 4.12–4.17]. However, a value of 1 W K^{-1} at 15 K has been reported in [4.18]. The main disadvantages of these switches are the large forces (typically 100 N) necessary to make adequate thermal contact and the heat generated when the contact is broken (typically 0.1–1 μJ N^{-1}). I will not discuss these switches in more detail here because they are being used less and less these days. Readers interested in mechanical thermal switches should consult the literature [4.1, 4.12–4.18].

4.2.2 Superconducting Heat Switches

In Sect. 3.3.4 we concluded that the thermal conductivity κ_s of a metal in the superconducting state can become very small because the number of electrons decreases exponentially with temperature; it can be orders of magnitude smaller than the thermal conductivity κ_n of the same material in the normal state (Fig. 4.1). Because some metals can easily be switched from the superconducting to the normal state by applying a magnetic field, we can build a "superconducting heat switch" as already mentioned in Sect. 3.3.4. Superconducting heat switches are the most common thermal switches at temperatures below about 1 K. Their advantages are that the heat flow in the open state is small, that they are very easy to switch, and that the switching ratio κ_n/κ_s can be very large; but for that we need $T < T_c/10$, which often means $T \ll 1$ K (Fig. 4.2). Very little heat is generated in the switching process if the design
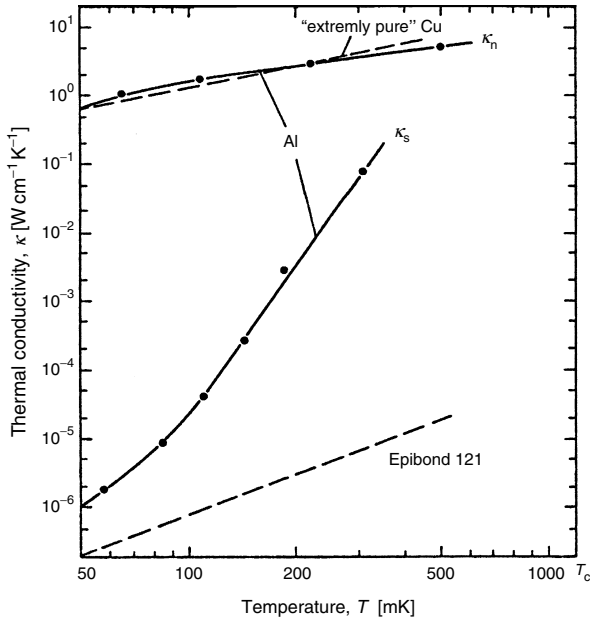
Fig. 4.1. Thermal conductivity κ of Al in the normal–conducting state (compared to κ of Cu) and in the superconducting state (compared to κ of the dielectric Epibond 121) at $T < 50\,\mathrm{mK}$ [4.19]
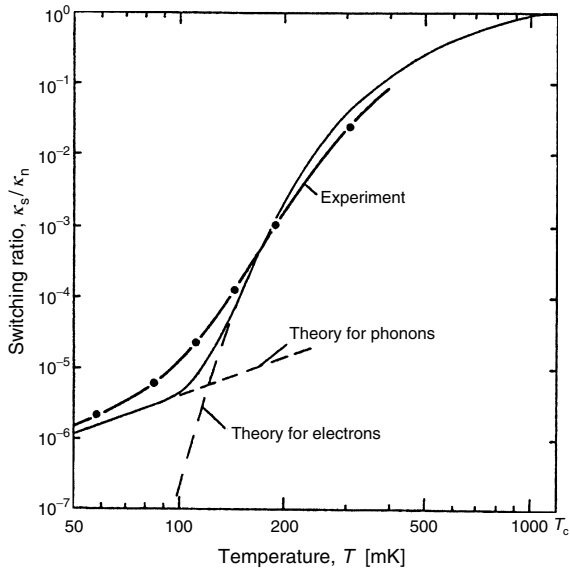

Fig. 4.2. Switching ratio $\kappa_\mathrm{s}/\kappa_\mathrm{n}$ of the thermal conductivity of Al compared to theoretical predictions [4.19]

ensures that eddy-current heating (Sect. 10.5.2) is small when the switching magnetic field is changing.

The quality of a superconducting heat switch is expressed by its switching ratio κ_n/κ_s. Here $\kappa_n \propto T$ whereas $\kappa_s \propto T \exp\left(-\Delta E/k_B T\right)$ for $T > T_c/10$ (from the remaining unpaired electrons) and $\kappa_s \propto (T/\theta_D)^3$ at $T < T_c/10$ (from the now dominating phonons), see Sect. 3.3.4. Hence one has the switching ratio

$$\frac{\kappa_n}{\kappa_s} = aT^{-2} \quad \text{for } T < 0.1\ T_c, \tag{4.1}$$

with a constant a of 10^2 – 10^3 for a properly designed switch (but see the comment at the end of this section).

Various designs of superconducting heat switches made from a variety of metals have been described in the literature [4.12, 4.19–4.28]. High-purity metals are used for a superconducting heat switch in order to make κ_n large. One should employ thin foils or wires (typically 0.1 mm) so that the mean free path of phonons – which is given by the sample dimensions for pure materials – and therefore κ_{ph} as well as eddy current heating during the field change become small. If $T < T_c/10$ and if we have high purity thin foils of a superconductor (so that phonons are only scattered at boundaries), then ideally

$$\frac{\kappa_n}{\kappa_s} \simeq 0.05 \left(\frac{\theta}{T}\right)^2, \tag{4.2}$$

for Al as an example [4.19].

The temperature dependence of the phonon conductivity (3.28) of a metal in the superconducting state and of the switching ratio (4.1, 4.2) should be used with caution. Recent measurements [4.28] of the thermal conductivity of massive pieces of superconducting Al (RRR $\geq 5,000$) have shown that $\kappa_{ph} \propto T^2$ for $10\,\text{mK} \leq T \leq 80\,\text{mK}$ (Fig. 4.3). Deviation from $\kappa_{ph} \propto T^3$ were reported earlier for Al, Nb and Ta [4.29, 4.30]. These deviations may be attributed to a scattering of phonons at dislocations (3.29) [4.31, 4.32], or to the glassy behavior (Figs. 3.21–3.23) observed recently for the acoustic properties of these metals [4.33]. The results for Al are particularly disturbing because the known properties of Al ($T_c = 1.18\,\text{K}$) indicate that for a superconducting heat switch it is superior to other candidates like Sn, In, Zn or Pb at $T \leq 0.1\,\text{K}$. A switch from the latter materials in the form of wires or foils can easily be constructed because of their low melting temperatures and good soldering properties. However, Al usually has a higher switching ratio (Fig. 4.2) because of its high κ_n and large Debye temperature ($\theta_D = 400\,\text{K}$), which makes κ_{ph} small. Aluminum is also easily available in very high purity (5 or 6 N; RRR $> 1,000$), has a convenient critical field (10.5 mT), good durability and is easy to handle. Of course, there is a serious contact problem due to the tenacious surface oxide on aluminum; various ways of solving this problem have been described in the literature. For a successful but elaborate
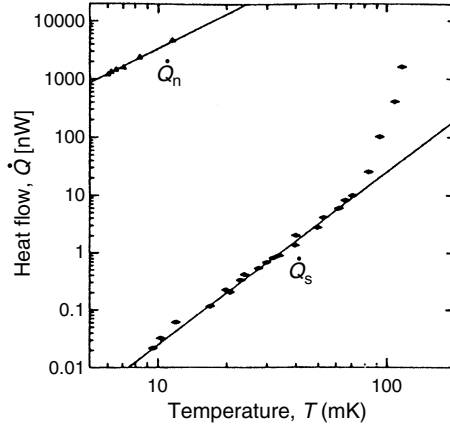
Fig. 4.3. Heat flow $\dot{Q}$ across an Al heat switch in the normal (▲) and superconducting (●) states. The lines correspond to $\dot{Q}_n \propto T^{-2}$ and $\dot{Q}_s \propto T^{-3}$. The thermal conductivity is $\kappa \propto (\dot{Q}T)^{-1}$, resulting in $\kappa_n \propto T$ and $\kappa_s \propto T^2$ at $T < 80\,\mathrm{mK}$ [4.28]

electroplating process see [4.6, 4.19], and procedures for welding Al to Cu or Ag have been described in [4.22–4.25]. In our laboratory recently contact resistances of $\leq 0.1\,\mu\Omega$ were achieved at $4.2\,\mathrm{K}$ by screwing well-annealed Ag screws into Al threads. The thread diameter had to be at least $6\,\mathrm{mm}$ in order for the necessary forces to be applied to the soft, annealed metals. Because of its larger thermal expansion coefficient the Al will shrink onto the Ag in the cooldown process (Fig. 3.17). Of course, for such a design high-temperature annealing does not help. The metals were chemically cleaned (HNO_3 for Ag; $22\mathrm{g}\,l^{-1}\mathrm{Na_3PO_4} + 22\mathrm{g}l^{-1}\mathrm{Na_2CO_3}$ at $T \geq 75°\mathrm{C}$, for A; several minutes), and annealed (5×10^{-5} mbar; $5\,\mathrm{h}$; $800°\mathrm{C}$ for Ag, $500°\mathrm{C}$ for Al). The best results for cold welding of Al to Cu are $\rho < 1\,\mu\Omega$ and RRR ≥ 150 for a pressure of $P \geq 100\,\mathrm{N\,mm^{-2}}$ applied at $500°\mathrm{C}$.

Often the behavior of a superconducting heat switch is deteriorated by frozen-in magnetic flux from the switching field, which may cause parts of the metal to remain in the normal state when the field is removed. This problem can be avoided by orientation of at least part of the metal perpendicular to the field (Fig. 4.4), so that the normal cores of trapped flux lines will not short-circuit the switch material, and/or by saw-tooth-like cycling of the field during its reduction. If a superconducting heat switch is used in a magnetic refrigerator (Chaps. 9 and 10), then in many cases a superconducting Nb shield should be placed around it to shield the switch from the changing fringe field of the demagnetization solenoid. The shape of the switch should be such that eddy current heating (10.28) produced while the switching field is changing will not cause heating effects, and that closed superconducting rings trapping flux are avoided (put slits perpendicular to the field into bulk Al) [4.28].
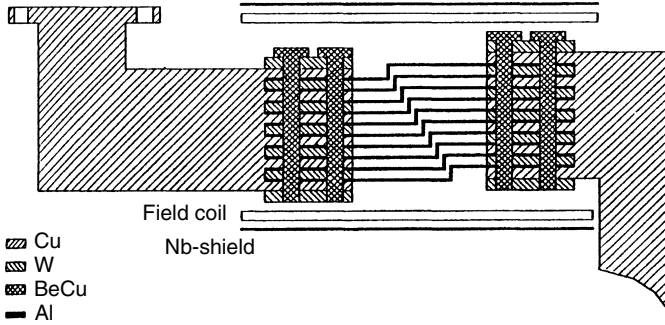
Fig. 4.4. Superconducting aluminum heat switch of the refrigerator in Bayreuth [4.34], see also Fig. 10.14. The superconducting foils are partly perpendicular to the magnetic field produced by the solenoid, thus avoiding that magnetic flux lines are able to penetrate into the switching foil along its entire length

4.3 Thermal Boundary Resistance

4.3.1 Boundary Resistance Between Metals

To achieve thermal equilibrium in a system becomes increasingly more difficult when the temperature is lowered, not only because the thermal conductivity of materials decreases with decreasing temperature but also because the thermal boundary resistance at the interface between two materials becomes increasingly important. If we have two different materials in contact and heat $\dot{Q}$ has to flow from one material to the other, for example in a cooling process, there will be a temperature step at the boundary between them. This temperature step is given by

$$\Delta T = R_{\mathrm{K}}\dot{Q}, \tag{4.3}$$

where R_{K} is the thermal boundary resistance, or Kapitza resistance, named after the Russian physicist P. Kapitza who discovered this thermal boundary resistance in 1941 for the case of liquid helium in contact with solids. This is still a problem which is not fully understood, at least for very low temperatures (Sect. 4.3.2). The boundary resistances between several materials are shown in Fig. 4.5.

Between metals the actual contact area often is only about 10^{-6} of the nominal contact area due to the microscopic irregularities of the opposing surfaces; the conductance therefore does not scale with the nominal contact area. The actual contact area can be considerably increased by the application of pressure close to the yielding stress of the materials. The thermal conductance across the boundary between the two metals is often proportional to the applied force used to press them together. The disadvantage of this procedure is a deformation of the lattice with a reduction in bulk conductivity. This problem is reduced by joining surfaces via diffusion welding because it uses high temperatures ($0.6\,T_{\mathrm{melting}}$, for example) annealing lattice defects.
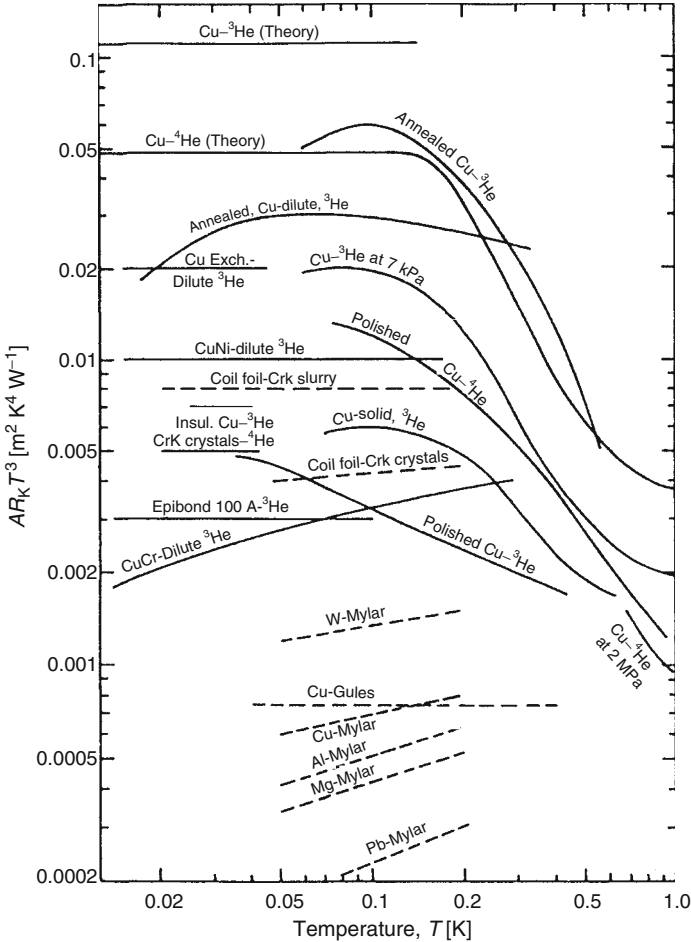
Fig. 4.5. Thermal boundary resistance R_K multiplied by AT^3 between liquid helium and various solids, and also between various metals and various dielectrics [4.12]. (This book provides references to the original literature); for more recent helium data see Fig. 4.9

The boundary resistance can be kept reasonably small, if the surfaces are clean, possibly gold-plated, and pressed together with a high force. We should then have an overlap of the electronic wave functions of the two metals, giving a good electric and thermal flow between them.

The heat transfer across the contact between two metals – similar or dissimilar – is a common problem in cryogenics. No unique solution can be found in the literature, even though it is full of recipes [4.1, 4.12, 4.35, 4.37]. In Sect. 3.2, I mentioned how important it is to correctly join two dissimilar materials, if good thermal contact is the goal. Predicting values for the conductance across a real joint is in general not possible; one has to resort to

experimental data. The largest amount of data on low-temperature contacts relates to contacts between two Cu surfaces, which are usually gold plated. Gold prevents the formation of an oxide layer on Cu; it may also play a role in enlarging the contact area because it deforms more easily than Cu. In [4.35], a detailed investigation of the thermal contact conductance of several gold plated Cu joints measured at about 0.4 K was reported. They were bolted together or clamped with torques between about 50 to 150 N cm. Most of the data fell into the range of 0.1–0.2 W/K at 1 K, and a linear temperature dependence was found, confirming electronic conductance.

Our own experience has shown that a well-designed demountable press contact between two gold plated or well-polished, clean metals can have a thermal resistance almost as small as a bulk, continuous part [4.19]. In order to achieve this, the surfaces have to be well prepared and strong enough bolts, made, for example, from hardened BeCu, have to be used. These are tightened in a controlled way until they almost yield, which supplies sufficient force for what is almost a cold weld to be produced between the two parts. This can rip up oxide layers and can then make an intimate metallic contact. Sometimes it helps if the joining surfaces are sprinkled with a fine soft Ag powder. As mentioned in Sect. 3.2, a washer with a very small expansion coefficient (e.g., W or Mo) improves the contact after cool down by taking advantage of the different thermal contractions. Rather good results have also been obtained with a joint of two tapered metals. Extremely small contact resistances of $10\,n\Omega$ at $4.2\,K$ between gold-plated Cu discs bolted together with 4 mm stainless-steel screws with a tightening torque of at least 4 Nm have been reported [4.36] (more typical, still good values are $0.1\,\mu\Omega$ at 4 K, [4.37]). The measured contact resistance was inversely proportional to the tightening torque on the screw. Salerno et al. [4.38] have reported that the addition of In foil or apiezon grease between the contact surfaces of Cu, Al, brass or stainless steel can result in improvements of up to an order of magnitude. Very small resistances have recently been achieved for electron-beam welded Cu–Ag joints with values of $0.2\,\mu\Omega\,mm^2$ at $4.2\,K$ [4.39].

The mechanical and electrical contact between two metals often is made by soldering them together. Unfortunately, most solders, in particular soft solders, become superconducting at low temperature (Table 4.1) and eventually behave like a dielectric with regard to thermal conductivity [4.1, 4.40–4.45] (Fig. 4.1); then one could just as well use a dielectric glue! Of course, this problem can be avoided if the solder joint can be exposed to a magnetic field high enough to suppress the superconducting state. Here, Ga with a melting temperature of 30°C and a critical field of only 2 mT ($T_c = 1.1\,K$) may be quite appropriate [4.46]. In some cases the low superconducting thermal conductivity may not reappear even after removal of the field because magnetic flux may be trapped in the solder, keeping enough of it in the normal state to provide good thermal contact. The transition temperatures to the superconducting state and melting temperatures of various solder alloys are given in Table 4.1. In some cases solder joints with non-superconducting Bi may be

Table 4.1. Melting temperatures T_m and superconducting transition temperatures T_c of some solders [4.1, 4.40–4.46]

solder	T_m [°C]	T_c [K]
12–14% Sn, 25–27% Pb, 50% Bi,		
10–13% Cd (Wood's metal)	70	8–9
50–52% In, 50–48% Sn	120	7.1–7.5
30–60% Sn, 70–40% Pb	257–183	7.1–7.8
97% Sn, 3% Ag	240	3.7
95.5% Sn, 3.5% Ag, 1% Cd	220	3.05
26% Sn, 54% Bi, 20% Cd	103	3.7
43% Sn, 57% Bi	140	2.25
82.5% Cd, 17.5% Zn	265	1–1.6
70% Au, 30% Sn (eutectic)	280	1.17
Ga	30	1.1
60% Bi, 40% Cd		<0.8
40% Ag, 19% Cu, 20% Cd, 21% Zn	610	<0.064
56% Ag, 22% Cu, 17% Zn, 5% Sn	650	<0.064
60% Ag, 30% Cu, 10% Sn	(700)	<0.057
50% Ag, 15.5% Cu, 16.5% Sn, 18% Cd	630	<0.057

appropriate [4.44]. These problems can be avoided by welding or using non-superconducting hard solders, but sometimes the alloy that is produced leads to a rather high thermal resistance at the interface between the two connected metals.

4.3.2 Boundary Resistance Between Liquid Helium and Solids

Acoustic Mismatch

Between dielectrics, for example a nonmagnetic dielectric in contact with liquid or solid helium, the transfer of energy can only occur via phonon transmission. We then have to match the acoustic properties of the two materials to optimize the transmission of phonons from one material to the other. The temperature step ΔT at the interface arises from the acoustic mismatch [4.12, 4.47–4.50] of the two materials, which I will treat in analogy to optics. In the following I will consider the case of transfering heat from liquid helium to another body with which it is in contact, because this is the most important case in low-temperature physics. For helium/solid interfaces the situation is particularly grave because acoustic impedances are $\rho_s v_s \approx 10^6 \, \mathrm{g \, (cm^2 \, s)^{-1}}$ for solids but $\rho_h v_h \approx 10^3 \, \mathrm{g \, (cm^2 \, s)^{-1}}$ for liquid helium. The importance of this heat transfer for low-temperature physics arises first of all from the fact that, except for magnetic refrigeration (Chaps. 9 and 10), all low-temperature refrigeration methods use helium as the working substance (Chaps. 5–8). Therefore, the cold produced by changing the thermodynamic state of helium has to be transferred to solid bodies to be useful.

Second, helium itself is a material of high scientific interest and in order to refrigerate it to the lowest possible temperatures by magnetic refrigeration, cold has to be transferred to it from a solid body, and its temperature has to be measured by a thermometer in intimate thermal contact with it. As a result, the thermal boundary resistance or energy transfer between liquid helium and solids is a matter of concern in a majority of low-temperature experiments, and it is a very interesting piece of physics in its own right.

If the velocity of phonons in helium is v_h and that in the solid is v_s, we have *Snell's law*

$$\frac{\sin \alpha_h}{\sin \alpha_s} = \frac{v_h}{v_s} \tag{4.4}$$

for the angles α at which the phonons cross the boundary. Because $v_h \approx 238\,\mathrm{m\,s^{-1}}$ for ^{4}He at $T \lesssim 1\,\mathrm{K}$ whereas $v_s \approx 3,000$ to $5,000\,\mathrm{m\,s^{-1}}$ for metals, the critical angle of incidence at which phonons from helium may enter the solid is very small,

$$\alpha_{crit} = \arcsin\left(\frac{v_h}{v_s}\right) \approx 3°. \tag{4.5}$$

The fraction of phonons hitting the interface that fall into the critical cone is

$$f = \frac{\pi \sin^2(\alpha_{crit})}{2\pi} = \frac{1}{2}\left(\frac{v_h}{v_s}\right)^2 \approx 2 \times 10^{-3}. \tag{4.6}$$

However, because of the difference in acoustic impedance $Z = \rho v$, not even all of these phonons are transmitted. The energy transmission coefficient under the assumption of perpendicular incidence of the phonons on the interface (which is well fulfilled because $\alpha_{int} \approx 3°$) is given by (with $Z_s \gg Z_h$)

$$t = \frac{4 Z_h Z_s}{(Z_h + Z_s)^2} \simeq \frac{4 \rho_h v_h}{\rho_s v_s} \simeq 3 \times 10^3. \tag{4.7}$$

Therefore only a fraction

$$ft = 2 \frac{\rho_h v_h^3}{\rho_s v_s^3} < 10^{-5} \tag{4.8}$$

of the phonons will enter the solid; hence the two bodies are rather well isolated from each other. The combination of acoustic mismatch and a small critical angle severely limits the energy exchange between helium and other materials.

The transmitted energy flux $\dot{Q}$ of phonons impinging on the contact area A per unit time is given by

$$\frac{\dot{Q}}{A} = \frac{\pi^2 k_B^4 T^4 \rho_h v_h}{30 \hbar^3 \rho_s v_s^3}. \tag{4.9}$$

The boundary resistance is then (for $\Delta T \ll T$)

$$R_K = \frac{\Delta T}{\dot{Q}} = \frac{dT}{d\dot{Q}} = \frac{15 \hbar^3 \rho_s v_s^3}{2\pi^2 k_B^4 T^3 A \rho_h v_h}. \tag{4.10}$$

In all the above equations, v_s is the transverse sound velocity.

A more rigorous consideration of the problem introduces corrections of order 2 depending on the materials properties. But the essential result is $R_K \propto (AT^3)^{-1}$; the boundary resistance increases strongly with decreasing temperature. This "acoustic mismatch prediction" is in reasonable agreement with most experimental data for $0.02\,\mathrm{K} < T < 0.2\,\mathrm{K}$ with typical values of $AR_K T^3 \simeq 10^{-2}\,\mathrm{m^2\,K^4\,W^{-1}}$ for liquid and solid helium in contact with metals, but deviates considerably both in the Kelvin temperature range (Figs. 4.5 and 4.6) and at $T < 10\,\mathrm{mK}$ (see "Acoustic Coupling Between Liquid Helium and Metal Sinters"). Another unexplained result is the observation that R_K seems to be about the same for ^{3}He and ^{4}He in the liquid as well as in the solid state at $T \approx 1\,\mathrm{K}$ (Fig. 4.6). Without question, the physics of the anomalously good thermal coupling at $T \geq 1\,\mathrm{K}$ is still not well understood, even though very detailed frequency-, angle-, and surface-condition-dependent studies have been performed [4.50–4.54] employing even modern high-frequency spectroscopic techniques [4.55]. The above results apply to annealed, bulk and clean metal surfaces. Of course, the experimental results depend strongly on the surface condition of the body in contact with helium, in particular surface roughness or mechanical damage of the surface. It can easily be
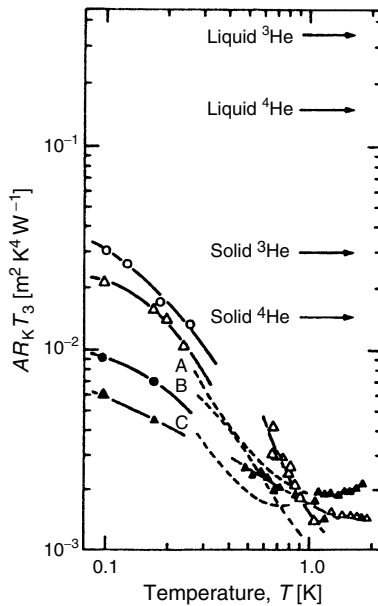

Fig. 4.6. Thermal boundary resistance R_K multiplied by AT^3 between ^{3}He or ^{4}He and copper as a function of temperature. (*open circle*): liquid ^{3}He; (*filled circle*): solid ^{3}He; (*open triangle*): liquid ^{4}He; (*filled triangle*): solid ^{4}He. The dashed curves A, B and C are for liquid ^{3}He, liquid ^{4}He and solid ^{3}He, respectively. The arrows at the right indicate the prediction from the acoustic mismatch theory (4.10) for an ideal Cu surface [4.50], where references to the original work are given

changed by an order of magnitude, for example, for ^{3}He–Cu interfaces from $AR_K T^3 = 4 \times 10^{-3}$ to $4 \times 10^{-2}\,\mathrm{m^2 K^4 W^{-1}}$ for $10\,\mathrm{mK} \leq T \leq 100\,\mathrm{mK}$ for different surface treatments (sand blasting, machining) [4.50–4.54] (Figs. 4.5 and 4.6). A rigorous treatment of the boundary resistance due to acoustic mismatch has to take into account the structure and properties of the solid and of helium near to the interface, and also the excitations there [4.47]. Surface excitations as well as a deviation from crystalline structure and the compression of helium resulting from the van der Waals attraction of the solid may influence the transmission coefficient for phonons.

The thermal boundary resistance $R_K \propto 1/(AT^3)$ is the most severe obstacle for establishing thermal contact between helium and other substances at $T < 1\,\mathrm{K}$. The common approach to improving this contact is by increasing the contact area A. This is mostly done by using heat exchangers made from sintered-metal powders; they will be discussed in Sects. 7.3.3 and 13.6. In addition, experiments reveal that the boundary conductance is considerably improved at $T < 20\,\mathrm{mK}$, as compared to the predictions of the acoustic mismatch prediction; this will be discussed in the next two Sections.

Acoustic Coupling Between Liquid Helium and Metal Sinters

In the preceding section on Acoustic Mismatch we saw that the mechanism of energy transfer across a metal-to-liquid interface is not completely understood; it is even less so if the metal is a sinter. Neither the electrons nor the single-particle helium excitations can cross the interface. The transfer has to be mediated by phonons and – in the case of ^{3}He – possibly by a magnetic coupling (see next section). As shown in the preceding section, the phonon coupling varies as T^3 and becomes very weak at low temperatures. One can compensate for this weakening by increasing the contact area A, i.e., by using metal sinters. Those used have surface areas of up to a few $100\,\mathrm{m^2}$ (Sects. 7.3.3 and 13.6). But this complicates the understanding even more because the vibrational modes of a sinter made of submicrometer particles will differ from the corresponding modes of the bulk metal. The lowest vibrational frequency ν for bulk phonons in a particle of diameter d is of order $(0.1\text{–}1)v_s/d$, where v_s is the velocity of sound in the particle [4.50, 4.56–4.59]. This corresponds to several gigahertz or $T \approx h\nu/3k_B \approx 10\,\mathrm{mK}$ for a particle of $d = 1\,\mathrm{\mu m}$. At higher frequencies the particle and its Kapitza resistance will behave bulk-like, whereas at lower frequencies the latter would increase exponentially. However, when metal particles are sintered they are connected by narrow elastic bridges (Sect. 13.6). This sponge with its elastic, open structure can have low-frequency continuum modes with a density of states which may be two orders of magnitude larger than the corresponding bulk density of phonon modes at $T \approx 10\,\mathrm{mK}$ [4.56–4.59]. These soft modes are assumed to couple well to
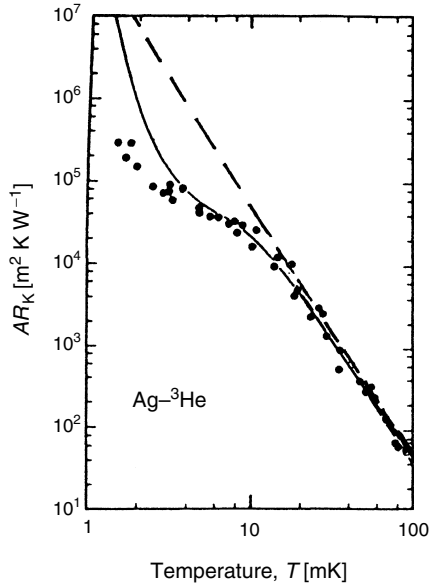
Fig. 4.7. Thermal boundary resistance R_K multiplied by the surface area A between liquid ^{3}He and a sinter of Ag particles. Experimental data from [4.60]. The dashed line represents the prediction of the acoustic mismatch theory (4.10) for bulk Ag. The full curve shows the prediction for a coupling of (zero) sound modes of liquid ^{3}He to soft modes with a characteristic energy of $15\,\text{mK}\,k_B$ of the Ag sinter [4.50]

the helium phonon modes with their small velocity of sound, as shown for a sinter of $1\,\mu\text{m}$ Ag powder and liquid ^{3}He in Fig. 4.7. As a further result, the boundary resistance will show a temperature dependence which is weaker than T^3 below a temperature where the dominant phonon wavelength becomes comparable to the size of the sinter particles; in [4.56] this dependence was found to be $R_K \propto T^{-1}$. Nakayama [4.50], in particular, has reviewed the heat transfer due to (zero) sound in liquid ^{3}He from ^{3}He to a metal sinter, the most important contact medium in the problem of energy transfer to liquid helium. But the situation is now more complicated than one would expect just from the change of the vibrational modes. The mean free paths of the electrons (whose influence on R_K is not understood) and phonons are limited by the sinter grain size and the mean free paths of the ^{3}He particles, and ^{3}He phonons are limited by the open dimensions of the sinter. The thermal resistance between excitations *in* the solid and/or *within* liquid helium can then become comparable to or even larger than the thermal boundary resistance at $T < 10\,\text{mK}$, and it certainly has to be taken into account when the thermal resistances inside of the liquid helium and/or inside of the metal sinter are considered. These effects have not yet been fully investigated.

Magnetic Coupling Between Liquid ^{3}He and Solids Containing Magnetic Moments

If the thermal coupling between liquid helium and solids were limited to phonon transfer or if the T^{-3} dependence of R_K continued to low millikelvin temperatures, it would require extremely large surface areas to refrigerate liquid ^{3}He into its superfluid states at $T < 2.5$ mK. However, in the middle of the 1960s a completely unexpected behavior of the thermal boundary resistance between liquid ^{3}He and the paramangetic salt CMN (Sect. 9.3) was reported [4.61–4.65]. Whereas above about 20 mK the data were in reasonable agreement with the acoustic mismatch theory, for 2 mK $\leq T \leq 20$ mK the thermal resistance between ^{3}He and powdered CMN was strongly reduced and *decreased* according to $R_K \propto T$ (Fig. 4.8). This result has inspired much research and provided the means of coupling ^{3}He well; and therefore cooling it into the low millikelvin temperature range, actually to 0.1 mK (see Table 10.2). Even though details of this enhanced thermal coupling are still not quite understood theoretically there is no doubt that a surface magnetic interaction between the nuclear magnetic moments of ^{3}He and electronic moments in the solid in contact with ^{3}He plays an essential part and short-circuits the acoustic mismatch [4.50, 4.66, 4.67]. The most convincing support for this interpretation comes from the observation that the enhanced coupling dramatically decreases if the solid surface is "plated" by a layer of (nonmagnetic) ^{4}He [4.62, 4.64, 4.65] (Fig. 4.8). The ^{4}He atoms coat walls preferentially
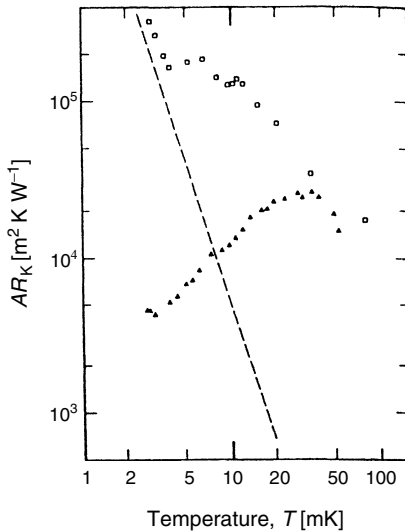

Fig. 4.8. Thermal boundary resistance R_K multiplied by the surface area A between the paramagnetic salt CMN (Sect. 9.3) and ^{3}He (*filled triangle*) and a 6% ^{3}He–^{4}He mixture (*open square*). The dashed line indicates the prediction of the acoustic mismatch theory, (4.10) [4.65]

because – due to their smaller zero-point energy compared to ^{3}He – they sit deeper in the van der Waals potential exerted by the wall. This interpretation is also supported by theoretical treatment of the magnetic dipole–dipole coupling between ^{3}He nuclear spins in the liquid and electronic spins in CMN, leading to $R_K \propto T$ [4.50, 4.66, 4.67], but the theory contains a number of significant assumptions [4.49, 4.50].

Later, qualitatively similar results –reasonable agreement with the acoustic mismatch theory in magnitude and temperature dependence for $20\,\mathrm{mK} < T < 100\,\mathrm{mK}$, and an enhanced thermal coupling at lower temperatures – was found for liquid ^{3}He in contact with various metals, particularly ("dirty") sinters. However, now the temperature dependence is $R_K \propto T^{-1}$, with typical values of $AR_K\,T \approx$ several 10^2 to $10^3\,\mathrm{m^2\,K^2\,W^{-1}}$ for sintered Cu and Ag powders or metal foils containing magnetic impurities [4.60, 4.68–4.73] (Figs 4.6, 4.7, and 4.9). Strong support for the magnetic coupling explanation is the
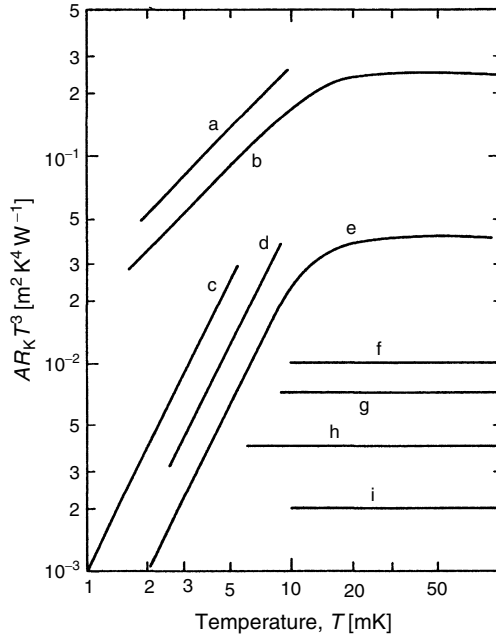

Fig. 4.9. Thermal boundary resistance R_K (multiplied by AT^3) between liquid ^{3}He or a liquid ^{3}He $-^4$He mixtures and various solids as a function of temperature. The data are for (**a**) mixture to 400 Å Ag sinter ($25\,T^{-2}$); (**b**) mixture to 700 Å Ag sinter ($16\,T^{-2}$ at $<10\,\mathrm{mK}$); (**c**) ^{3}He to 700 Å Ag sinter ($1,000\,T^{-1}$); (**d**) ^{3}He to 400 Å Ag sinter ($470\,T^{-1}$); (**e**) ^{3}He to $1\,\mu\mathrm{m}$ Ag sinter ($200\,T^{-1}$ at $<10\,\mathrm{mK}$); (**f**) mixture to CuNi ($10^{-2}\,T^{-3}$); (**g**) mixture to brass ($7 \times 10^{-3}\,T^{-3}$); (**h**) mixture to $7\,\mu\mathrm{m}$ thick Kapton foils ($4 \times 10^{-3}\,T^{-3}$); (**i**) mixture to Teflon tubing with 0.1 mm wall thickness ($2 \times 10^{-3}\,T^{-3}$); (the data in brackets are AR_K) [4.73, this paper gives listings of the original works]

apparent absence of a contribution from the electron–phonon resistance in the metal and from the phonon–^{3}He-quasiparticle resistance in the liquid [4.50]; this indicates a direct ^{3}He spin-metal spin/electron coupling bypassing the phonons.

The possibility of changing the Fermi temperature T_F of liquid ^{3}He–^{4}He mixtures by changing their concentration (7.23a) offers an opportunity to gain more insight into the coupling between ^{3}He–^{4}He mixtures and solids. Indeed, for this combination, too, an enhanced coupling was found [4.72–4.77], but now with a dependence on T_F, with typical values $AR_K \approx 6T^{-2}T_F^{-1}$ m^2 K W^{-1} at $T \leq 20$ mK [4.50, 4.76, 4.77]. The T^{-2} dependence is obtained by assuming a magnetic dipole coupling between the nuclear magnetic moments of ^{3}He and the electronic magnetic impurities moment S localized in the solid surface [4.50]. The dependence on the Fermi temperature T_F of the mixtures indicates the quantum and magnetic character of the coupling. For saturated ^{3}He–^{4}He mixtures (Chap. 7), values of $AR_K = (12$–$35)T^{-2}$ m^2 K W^{-1} have been reported [4.72–4.77].

These observations were far from understood when the first review article on the thermal boundary resistance at $T < 0.1$ K was written in 1979 [4.49]. Substantial experimental and theoretical effort enabled Nakayama to present a more concise picture on the problem in 1989 [4.50] (Fig 4.10). These two comprehensive reviews should be consulted for further details and, in particular, for references to other works in the field. The situation still cannot be considered as understood and many more experiments on the thermal boundary resistance, particularly at $T \leq 20$ mK, seem to be necessary. For example, there are conflicting results on the pressure and magnetic field dependence of R_K [4.78–4.80]. Furthermore, the influence of the changing structure of helium near to the substrate resulting from the van der Waals attraction (localization, compression, preferentially ^{4}He in the case of mixtures) is an interesting topic. Finally, the question of whether the magnetic coupling results from electronic magnetic moments in the metal or is due to absorbed impurity layers, particularly various paramagnetic oxides with localized moments [4.50], is of interest. A relation between the magnetic properties of Ag sinters containing a few ppm of magnetic impurities and their thermal boundary resistance to liquid ^{3}He has been discussed in [4.81] stressing the importance of a "magnetic channel" for the heat transfer. The role of conduction electrons for R_K also remains to be more thoroughly investigated.

Even though much remains to be measured and understood, the Kapitza-resistance problem can clearly be divided into three distinct temperature regimes:

(a) Above 1 K: R_K is essentially the same for liquid and solid ^{3}He and ^{4}He; it is at least an order of magnitude smaller than predicted by the acoustic mismatch theory, and it is not understood.
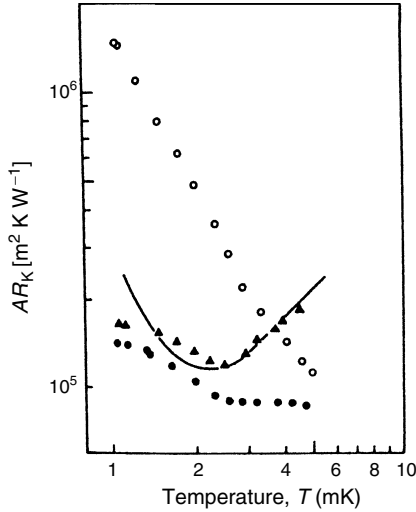
Fig. 4.10. Thermal boundary resistance R_K multiplied by the surface area A between liquid ^{3}He and a sinter of Ag particles. The experimental data for zero magnetic field (*filled circle*) and for a measurement in $0.385\,T$ (*open circle*) are from [4.78]. The field is assumed to suppress the magnetic contribution to R_K, leaving only the acoustic channel for heat transfer. Therefore the difference between the two sets of experimental data should given the magnetic contribution (*filled triangle*) to R_K. The solid line represents the theoretical prediction for this magnetic contribution [4.50]

(b) For $20\,\text{mK} \leq T \leq 100\,\text{mK}$: $R_K \propto T^{-3}$ and behaves as predicted by the acoustic mismatch theory if well characterized, clean, bulk metallic surfaces are used.

(c) At $T \leq 10\,\text{mK}$: $R_K \propto T^{-2}$ or T^{-1} between liquid ^{3}He or helium mixtures and metals, and is again much smaller than predicted by the acoustic mismatch theory; here a magnetic dipole coupling between the ^{3}He nuclear moments and electronic moments in (or on) the solid together with a coupling of helium phonon modes to soft vibrational modes, if a sintered metal is used, seem to determine the energy flux. These effects have turned out to be extremely important for refrigeration in the low millikelvin and sub-millikelvin temperature ranges.

Problems

4.1. Calculate the temperature at which the contributions from phonons and from electrons to the switching ratio of a superconducting heat switch of Al become equal (Fig. 4.2; take material parameters from Table 10.1).

4.2. The difference in entropy of the superconducting and normal–conducting state at the transition of a superconducting metal is $S_s - S_n = (V/4\pi) B_c(dB_c/dT)$. Calculate the latent heat occuring when a superconducting heat switch is changed from one state to the other.

4.3. Deduce (4.9).

4.4. To which temperature can one refrigerate a sample of liquid ^{3}He in a sintered heat exchanger of $10\,\mathrm{m}^2$ if the liquid releases $\dot{Q} = 0.1\,\mathrm{nW}$?